Available online at www.sciencedirect.com
ScienceDirect
Advances in Water Resources 31 (2008) 1444–1455
Advances in Water Resources
www.elsevier.com/locate/advwatres

The NAFE'06 data set: Towards soil moisture retrieval at intermediate resolution

Olivier Merlin [a,*], Jeffrey P. Walker [a], Jetse D. Kalma [b], Edward J. Kim [c], Jorg Hacker [d], Rocco Panciera [a], Rodger Young [a], Gregory Summerell [e], John Hornbuckle [f], Mohsin Hafeez [g], Thomas Jackson [h]

[a] Civil and Environmental Engineering, The University of Melbourne, Australia
[b] School of Engineering, University of Newcastle, Australia
[c] National Aeronautics and Space Administration, Goddard Space Flight Center, USA
[d] Flinders University/Airborne, Research Australia, Australia
[e] Department of Environment and Climate Change, Australia
[f] Commonwealth Scientific and Industrial Research Organisation, Land and Water, Australia
[g] International Centre of Water for Food Security, Australia
[h] United States Department of Agriculture, USA

Received 5 July 2007; received in revised form 17 December 2007; accepted 23 January 2008
Available online 12 February 2008

Abstract

The National Airborne Field Experiment 2006 (NAFE'06) was conducted during a three week period of November 2006 in the Murrumbidgee River catchment, located in southeastern Australia. One objective of NAFE'06 was to explore the suitability of the area for SMOS (Soil Moisture and Ocean Salinity) calibration/validation and develop downscaling and assimilation techniques for when SMOS does come on line. Airborne L-band brightness temperature was mapped at 1 km resolution 11 times (every 1–3 days) over a 40 by 55 km area in the Yanco region and 3 times over a 40 by 50 km area that includes Kyeamba Creek catchment. Moreover, multi-resolution, multi-angle and multi-spectral airborne data including surface temperature, surface reflectance (green, read and near infrared), lidar data and aerial photos were acquired over selected areas to develop downscaling algorithms and test multi-angle and multi-spectral retrieval approaches. The near-surface soil moisture was measured extensively on the ground in eight sampling areas concurrently with aircraft flights, and the soil moisture profile was continuously monitored at 41 sites. Preliminary analyses indicate that (i) the uncertainty of a single ground measurement was typically less than 5% vol. (ii) the spatial variability of ground measurements at 1 km resolution was up to 10% vol. and (iii) the validation of 1 km resolution L-band data is facilitated by selecting pixels with a spatial soil moisture variability lower than the point-scale uncertainty. The sensitivity of passive microwave and thermal data is also compared at 1 km resolution to illustrate the multi-spectral synergy for soil moisture monitoring at improved accuracy and resolution. The data described in this paper are available at www.nafe.unimelb.edu.au.
© 2008 Elsevier Ltd. All rights reserved.

Keywords: Soil moisture; Airborne experiment; L-band radiometry; Multi-spectral; Synergy; Calibration/validation; Downscaling; Assimilation

1. Introduction

Soil moisture variability controls catchment-scale hydrological processes [27] and impacts meso-scale atmospheric circulations [22] at time scales ranging from the inter-storm period to the season. Soil moisture estimates at high spatial and temporal resolutions are therefore critical in hydrology, meteorology, climate change studies and related disciplines.

Passive radiometry at L-band is one of the most promising techniques for measuring and monitoring soil

* Corresponding author. Tel.: +61 3 8344 5628.
E-mail address: omerlin@unimelb.edu.au (O. Merlin).

0309-1708/$ - see front matter © 2008 Elsevier Ltd. All rights reserved.
doi:10.1016/j.advwatres.2008.01.018

moisture at global scale [7,24]. A number of field experiments around the world (e.g. [3,6,14,18,19]) have demonstrated the high sensitivity of L-band land surface emission to moisture status, and the possibility of inferring near-surface soil moisture from these data. The Soil Moisture and Ocean Salinity (SMOS) mission [8], scheduled for launch in 2008, will be the first satellite dedicated to this application that incorporates this approach. The multi-incidence and dual-polarisation capabilities of the SMOS radiometer will allow novel approaches for the retrieval of 0–5 cm soil moisture every 2–3 days at $\sim$ 40 km resolution globally [29].

Retrieval at global scale requires development and testing of radiative transfer models over a range of surface conditions. To date, L-band soil moisture retrieval algorithms have been developed mainly against data collected by ground-based radiometers [28], allowing fine scale studies of the surface emission over different vegetation and soil types. Consequently, these models need to be tested for a wider range of land surface conditions and at lower resolution, to include the sub-pixel heterogeneity of land cover and land use that would occur at 40 km scale. However, the validation of $\sim$ 40 km resolution retrievals is not a trivial task. Recent studies have tackled the issue of upscaling point-scale measurements by identifying catchment-scale representative stations [5] and combining ground measurements with a spatially distributed land surface model [2], but the performance of these approaches is site-dependent. Actually, the development and testing of the retrieval models requires data at an intermediate resolution, so as to account for the natural heterogeneity of land surfaces at the satellite scale and yet be comparable with the representative scale of ground measurements. Such intermediate data can only be obtained from aircraft measurements.

The spatial resolution of airborne data typically ranges from 50 m to 1 km [6,14]. This intermediate spatial scale can be used to bridge the gap between point-scale measurements and satellite observations. Specifically, airborne data can be used to assess the models developed from ground-based data and develop parameterizations which include the sub-pixel surface heterogeneity. Moreover, aircraft data at L-band can cover several satellite footprints in a day. This allows for simulating several satellite pixels and testing downscaling [9,11] and assimilation [4,25] techniques with data that are consistent with satellite scales, before application with real satellite data.

This paper describes the data collected during the National Airborne Field Experiment 2006 (NAFE'06), conducted from 30 October to 20 November 2006 in the Murrumbidgee catchment, located in southeastern Australia. The primary objective of NAFE'06 was to provide airborne data at intermediate resolution for development and testing of SMOS scale soil moisture retrieval, downscaling and assimilation over two $\sim$ 40 km size sites. The surface conditions varied from extremely dry at the beginning of the campaign to quite wet in the near-surface, with significant rainfall events on 2 and 13 November of about 10 and 15 mm respectively. An overview of the study sites, experimental design and data set is presented. Preliminary results from NAFE'06 are also provided to assess the accuracy and sensitivity of ground, airborne and satellite data at the intermediate spatial scale of 1 km.

2. Study area description

The NAFE'06 campaign has been undertaken across three separate regions of the Murrumbidgee catchment (Fig. 1): (i) Yanco, (ii) Kyeamba Creek and (iii) Yenda. Climate in the Murrumbidgee catchment varies from semi-arid in the west to alpine in the east. The soil moisture monitoring networks operating in the study area are listed in Table 1.

2.1. Yanco area (3600 km^2)

The Yanco area is a 60 km by 60 km area located in the western flat plains of the Murrumbidgee catchment. Approximately one third of the Yanco area is occupied by the Coleambally Irrigation Area (CIA), an agricultural area that contains more than 500 farms. The principal summer crops grown in the CIA are rice, maize, and soybeans, while winter crops include wheat, barley, oats, and canola. The 13 soil moisture monitoring sites in the Yanco area are evenly divided between the three main land uses in the region: irrigated cropping, dryland cropping, and grazing.

In November, rice crops are usually flooded with about 30 cm of irrigation water [23]. An important component of the NAFE'06 design was to provide L-band data over the CIA to assess the impact of standing water on brightness temperature and soil moisture retrieval.

2.2. Kyeamba Creek (600 km^2)

Kyeamba Creek is a third-order catchment feeding the Murrumbidgee River. Land use is dominated by cattle grazing, limited sheep grazing and some irrigated cropping. The catchment is equipped with 14 soil moisture monitoring stations and a 3D Eddy correlation flux tower at K10 (Fig. 1). In addition, there are eight soil moisture stations at a single farm (O'Briens in Fig. 1) of the Livingstone subcatchment, operated by Department of Environment and Climate Change (DECC) in Wagga Wagga. Soil types and landforms occurring in the Livingstone subcatchment are reflective of the main soils and landforms in the broader Kyeamba catchment.

2.3. Yenda (0.26 km^2)

The Yenda site is an experimental farm operated by Commonwealth Scientific and Industrial Research Organisation (CSIRO) in Griffith, located 40 km north of the Yanco area. Measurements undertaken in two adjacent vineyards (14 and 12 ha) include: sap flow of individual vines, soil moisture and soil tension at 10 locations, and

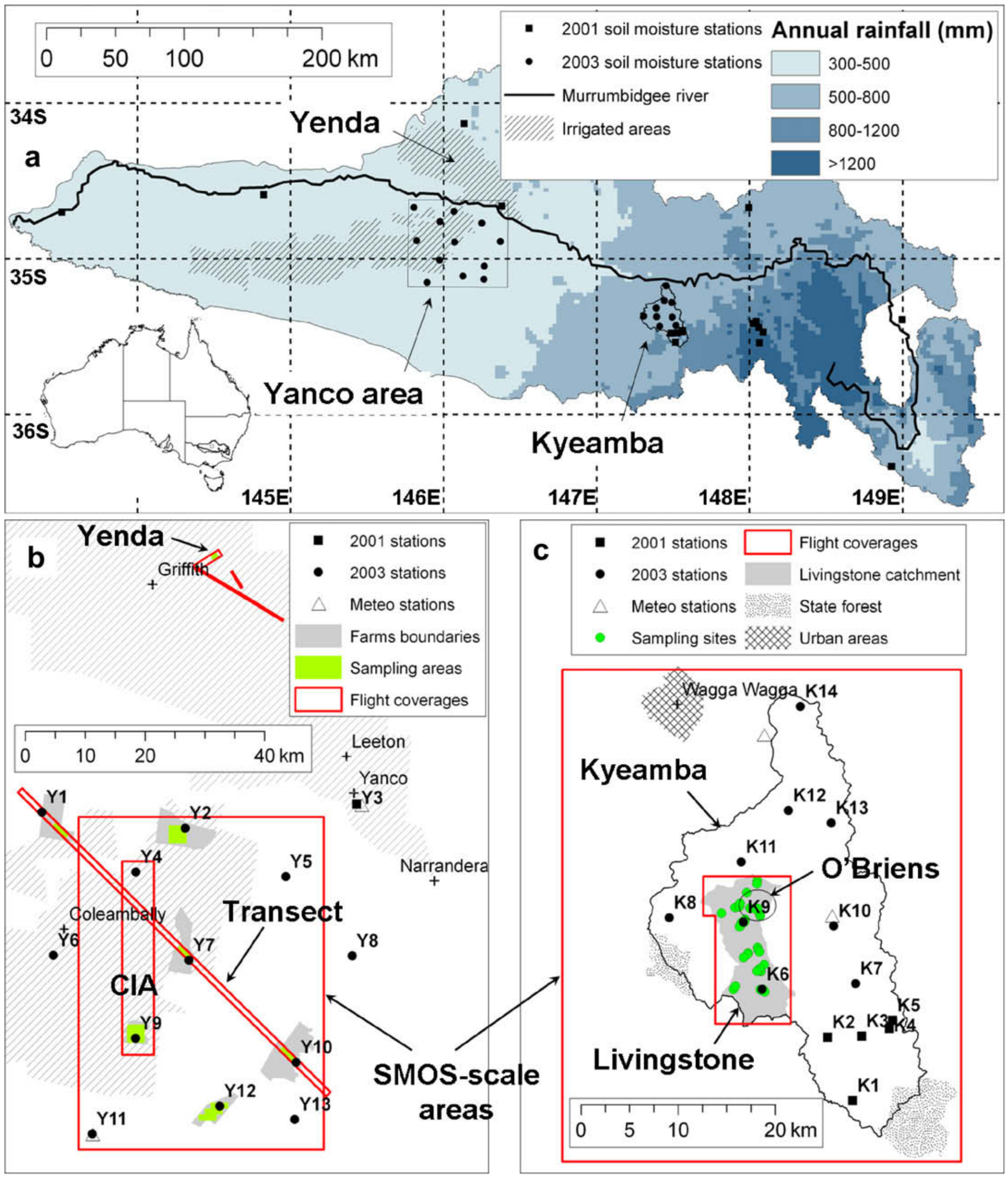

Fig. 1. Overview of the Murrumbidgee River catchment, soil moisture monitoring sites, NAFE'06 study areas, focus farms, campaign monitoring and flight coverages.

Table 1
Soil moisture monitoring networks

Network	Extent	Area (km^2)	Number of stations
OzNet	Murrumbidgee catchment	80000	38
OzNet	Yanco area	3600	13
OzNet	Kyeamba catchment	600	14
Livingstone	Livingstone catchment	47	10 (8 DECC + 2 OzNet)
DECC	O'Briens Creek	1	8
CSIRO	Yenda vines	0.26	10

Bowen ratio at three locations. Spatial ground-based electromagnetic measurements of soil salinity have also been taken using a Geonics EM38 meter.

3. Data description

The NAFE'06 data set is composed of airborne data collected on 16 days over the Yanco area, 4 days over Kyeamba and 2 days over Yenda, with coincident ground measurements at eight focus sampling areas to complement the permanent ground monitoring networks.

3.1. Airborne data

A total of approximately 100 flight hours with six different flight types were conducted during the 3-week campaign. Flight coverages are illustrated in Fig. 1 and a summary of the flight schedule, flight types, and airborne data types/extent/resolution is provided in Table 2.

3.1.1. Airborne instruments

The Polarimetric L-band Multi-beam Radiometer (PLMR) measures both V and H polarisations using a single receiver with polarisation switching at incidence angles of ±7°, ±21.5° and ± 38.5°. The instrument can be mounted in either across track (image) or along track (multi-angle) configurations. The accuracy of the PLMR was estimated to be higher than 2 K and 3 K in the H and V polarisation, respectively [14]. The PLMR data have been processed for incidence angle and beam location on the ground taking into account aircraft position, attitude and ground topography. Other airborne instruments included a thermal imager for surface skin temperature, tri-spectral line scanner (TSLS) for NDVI, full waveform lidar for construction of both DSM (Digital Surface Model) and DTM (Digital Terrain Model) as well as the analysis of the structure of vegetation, and digital camera for visible data. The thermal imager was flown with the PLMR on all flights to provide simultaneous skin temperature that will be used to compute effective temperature in the soil moisture retrieval algorithm. The TSLS, lidar and visible camera were flown together once only over a selected region of the three study sites.

Table 2
Airborne data summary per flight type

Flight type	Coverage (schedule)	Data and resolution
Satellite-scale:	Yanco (11 times, every 1–3 days)	PLMR 1000 m
Mixed pixel retrieval	Kyeamba (3 times)	Thermal 20 m
Downscaling and assimilation		
Catchment-scale:	Livingstone (4 times, once a week)	PLMR 250 m/1000 m
Water balance	Kyeamba (3 times)	Thermal 5 m/20 m NDVI 1.5 m Photos 0.2/1 m
Paddock-scale:	Yenda (twice)	PLMR 50 m
Crop stress estimation		Thermal 1 m NDVI 1.5 m Lidar 0.2 m Photos 0.2 m
Multi-angle:	Transect 6 a.m. (3 times, once a week)	PLMR 500 m
Multi-angle retrieval	Transect 6 p.m. (3 times, once a week)	Thermal 10 m
Multi-spectral:	Transect (6 times, twice a week)	PLMR 50 m/250 m
Multi-sensor retrieval	Livingstone (4 times, once a week)	Thermal 1 m/5 m
	Area in CIA (3 times, once a week)	NDVI 1.5 m
	Yenda (twice)	Lidar 0.2 m Photos 0.2 m/1 m
Irrigation:	Area in CIA (3 times, once a week)	PLMR 50 m/250 m/1000 m
Standing water impact on retrieval	Transect (6 times, twice a week)	Thermal 1 m/5 m/20 m

3.1.2. Satellite-scale flights (Yanco and Kyeamba)

The L-band brightness temperature was mapped at 1 km resolution 11 times over a 40 km by 55 km area in Yanco and three times over a 40 km by 50 km area including the Kyeamba catchment. This simulated two ∼ 40 km scale satellite pixels over mixed land use, including standing water in Yanco and the city of Wagga Wagga in Kyeamba for testing mixed pixel retrieval. This also provided data at a spatial resolution consistent with MODerate resolution Imaging Spectroradiometer (MODIS) data for testing downscaling techniques based on multi-spectral satellite data. Moreover, the temporal frequency over Yanco (1–3 days) was consistent with SMOS repeat time (2–3 days) for testing root-zone retrieval from assimilation into land surface models.

The PLMR flights were scheduled to maximize the number of concurrent MODIS overpass. Table 3 lists the days when 1 km resolution PLMR data were acquired within ±2 h with MODIS data, together with the percent of cloud cover present in the MODIS products available and the MODIS zenith view angle. Of the 14 days, 9 days had more than 88% cloud free including 5 days with both MODIS/Terra (10 a.m.) and MODIS/Aqua (1 p.m.) overpass.

Fig. 2 presents the 1 km resolution images of H-polarised brightness temperature corrected to 7° incidence angle. For Yanco, dry downs resulting from the rainfall events on 2–3 November and 12–13 November are readily seen by the 11 flights. Note that irrigation in the CIA can be observed on 31 October and 4 November, due to its strong decreasing effect on L-band brightness temperature. This period corresponds to initial bay filling and permanent ponding of rice in the area.

3.1.3. Multi-angle flights (Transect)

For this flight type, the PLMR was mounted in the along track configuration to collect multi-angular data for SMOS algorithm development. The transect (shown

Table 3
MODIS overpass time, cloud cover and mean zenith angle over Yanco and Kyeamba, on the 1 km resolution PLMR flight days.

Date	Julian day	1 km PLMR	10 a.m. Terra	1 p.m. Aqua
Monday October 30	303	Kyeamba	–	6% (18°)
Tuesday October 31	304	Yanco	12% (30°)	0 (51°)
Thursday November 2	306	Yanco	100%	100%
Friday November 3	307	Yanco	0 (30°)	3% (1°)
Saturday November 4	308	Yanco	–	7% (30°)
Sunday November 5	309	Yanco	0 (20°)	3% (60°)
Monday November 6	310	Kyeamba	–	34% (23°)
Tuesday November 7	311	Yanco	6% (36°)	12% (55°)
Thursday November 9	313	Yanco	1% (24°)	0 (47°)
Monday November 13	317	Yanco	–	58% (24°)
Tuesday November 14	318	Yanco	8% (42°)	100%
Thursday November 16	320	Yanco	34% (30°)	95% (52°)
Saturday November 18	322	Yanco	0 (19°)	50% (42°)
Monday November 20	324	Kyeamba	–	94% (34°)

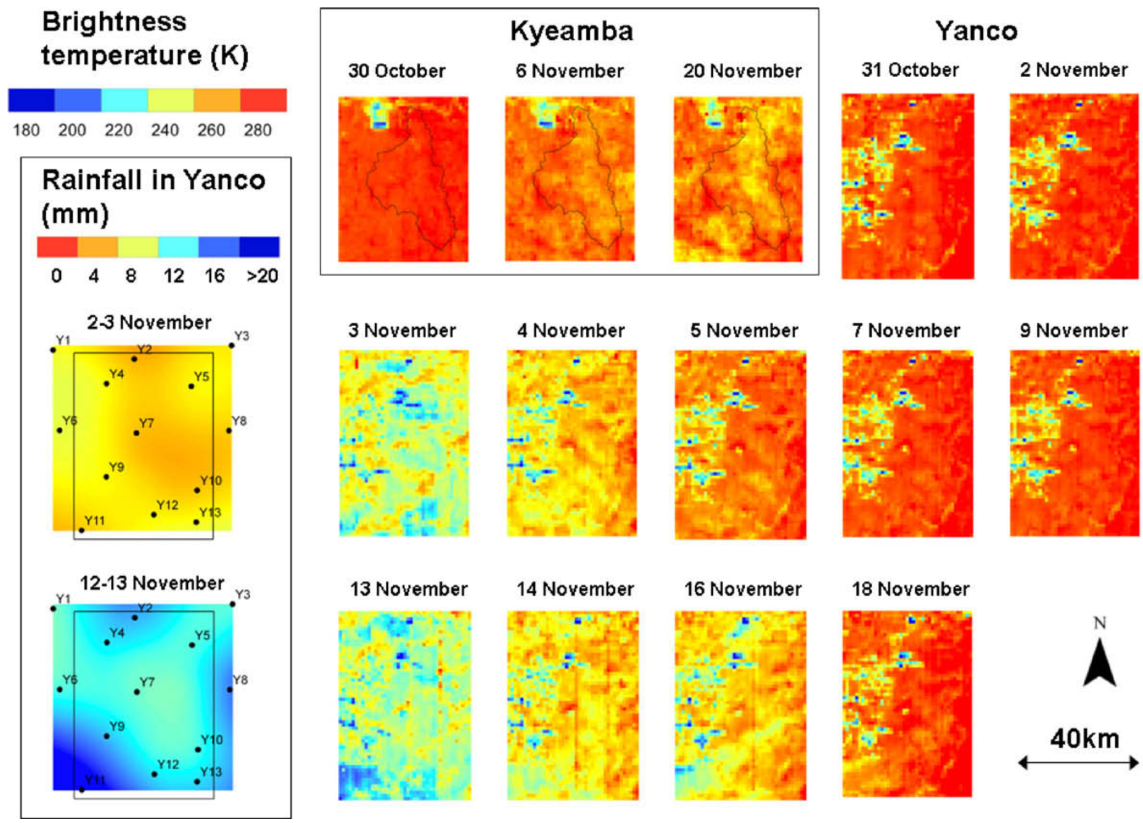

Fig. 2. Illustration of wetting and drying experienced during the campaign seen by the L-band brightness temperature. The spatial distribution of rainfall events 2–3 and 12–13 November interpolated from the rain gauge network is consistent with the L-band data on 3 and 13 November.

Fig. 1) was flown twice a week, alternatively at 6 a.m./6 p.m., so that both SMOS overpass times can be tested.

3.1.4. Multi-spectral flights (Transect, CIA, Livingstone and Yenda)

Multi-spectral airborne data including L-band brightness temperature, skin temperature, surface reflectance, lidar data and aerial photos were collected over selected areas: a 75 km by 1 km area along the multi-angle transect line, a 3 km by 32 km area in the CIA, Livingstone and Yenda. Fig. 3 presents an example of airborne data collected in the optical and microwave domains over the transect. These complementary information on the surface state illustrate the possible synergism of multi-spectral remote sensing data for retrieving land surface parameters including soil moisture.

3.1.5. Irrigation flights (CIA)

The L-band brightness temperature was collected at 250 m resolution over a 3 km by 32 km area in the CIA. These flights were undertaken on the same day as the satellite-scale flights to assess the impact of standing water on L-band observations at scales ranging from 250 m to 1 km, and repeated once a week to monitor new bay fillings during the 3-week campaign. Fig. 4 illustrates the multi-resolution data acquired over the CIA on 14 November for 1 km and 250 m data, and on 15 November for 50 m data. The effect of standing water is clearly visible on the images at 250 m and 50 m resolution where brightness temperature drops below 150 K over rice crops.

3.1.6. Catchment-scale flights (Kyeamba)

The L-band brightness temperature was mapped at 250 m resolution over a 7 km by 15 km area that includes the Livingstone subcatchment on 4 days. These flights were undertaken on the same day as the satellite-scale flights over Kyeamba to investigate catchment-scale water balance studies and scaling issues.

3.1.7. Paddock-scale flights (Yenda)

Multi-spectral data at high-resolution were collected twice over a 3 km by 0.8 km area in Yenda. These data will be used to investigate the water flux and solute interactions in high spatial detail from heterogenous (i.e. row crop) irrigation systems.

3.2. Ground data

The ground data set are composed of (i) spatial near-surface soil moisture measurements in eight focus sampling areas covering different scales, (ii) continuous measurements of a range of variables from the ground monitoring networks and (iii) other ancillary data that are required in the soil moisture retrieval algorithms.

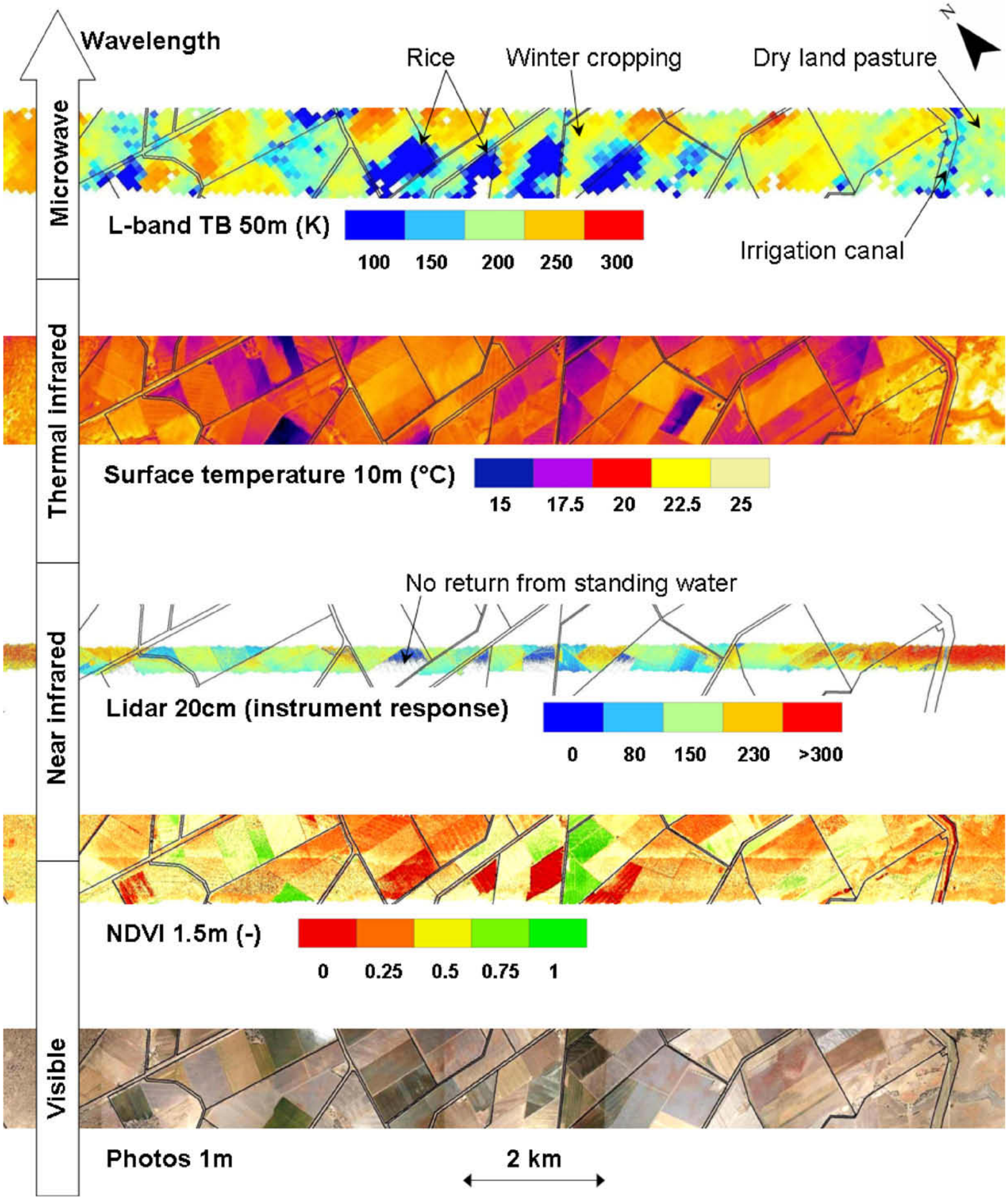

Fig. 3. Sample of multi-spectral/multi-resolution airborne data acquired on 3 November over the transect in Yanco.

3.2.1. Spatial soil moisture data

The location and coverage of soil moisture sampling sites and areas discussed below are shown in Fig. 1. For logistical reasons, the ground teams in Yanco, Kyeamba and Yenda operated independently with different sampling strategies.

In Yanco, the 0–5 cm soil moisture measurements were made using the Hydraprobe Data Acquisition System (HDAS, [13]). Spatial measurements were made over a 3 km by 3 km area of 3 farms on a 250 m resolution grid during 1 km "satellite-scale" flights and over a 3 km by 1 km area of a separate three farms on a predominantly 50 m resolution grid during PLMR "multi-angle" flights. The calibration approach described in [20] was applied to the about 17 000 HDAS roving measurements [12]. Images of the spatial data collected in Yanco on two days of the experiment (13 and 15 November) are presented in Fig. 5. The impact of natural variability in dryland farms

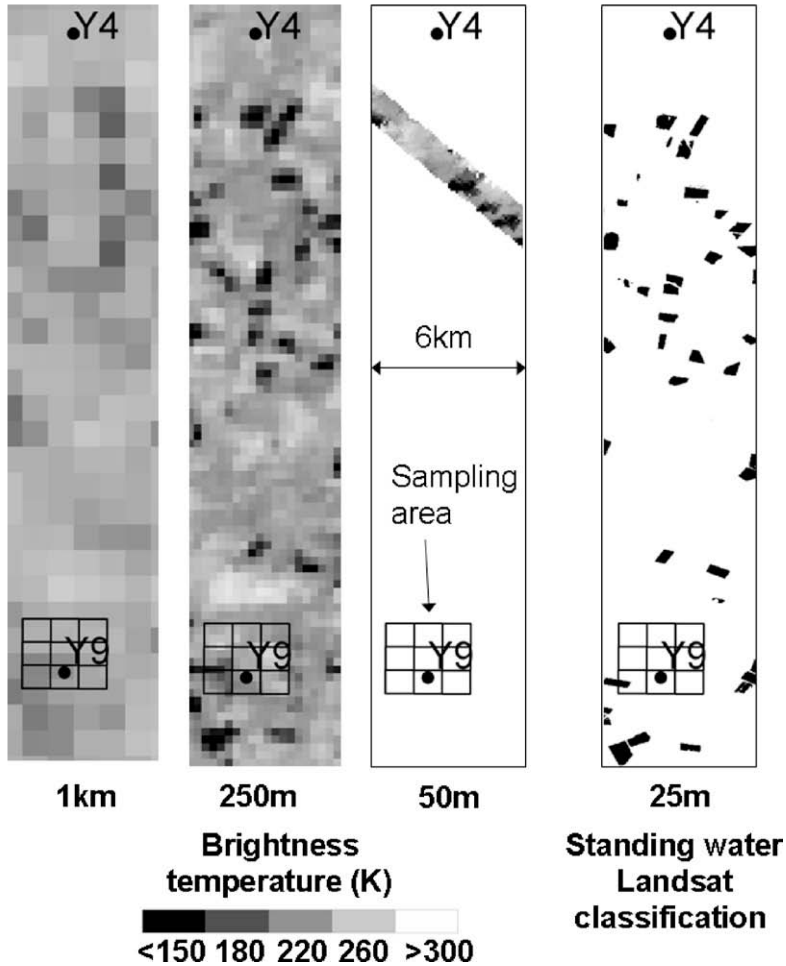

Fig. 4. Sample of multi-resolution (1 km, 250 m and 50 m) PLMR data over the medium resolution area of the Coleambally Irrigation Area sampled to explore standing water impacts on brightness temperature measurements. For comparison, a standing water classification was derived at 25 m resolution from a Landsat image.

Y2, Y7 and Y10, and of irrigation in cropping farms Y1, Y9 and Y12 can be observed on 0–5 cm soil moisture.

In Kyeamba, the 0–5 cm soil moisture was measured with a Theta probe at 35 locations across the 47 km^2 Livingstone catchment. The 35 field sites were selected to represent the major landforms by soil type in the Livingstone Creek [21].

In Yenda, the 0–5 cm soil moisture was measured with the gravimetric approach. Six volumetric samples were collected at each node of a 50 m-resolution grid covering the two vine paddocks (26 ha).

3.2.2. Ancillary data

The soil moisture sites of the Murrumbidgee network (OzNet) measure the soil moisture at 0–5 cm (or 0–7 cm for the older sites), 0–30 cm, 30–60 cm and 60–90 cm with CS616 (CS615 for older sites) water reflectometers, precipitation using a tipping bucket rain gauge, and soil temperature. A schematic diagram of the stations is presented in Fig. 6. Calibration of the soil water reflectometers is based on the approach of [26] with a combination of laboratory and field data [15]. Additionally, six stations were set up for the duration of the experiment (NAFE stations) to monitor near-surface soil temperature at 1 cm, 2.5 cm and 5 cm depth, ground-based thermal surface temperature, and leaf wetness (see Fig. 6). The primary purpose of this monitoring was to derive the effective microwave soil temperature from thermal infrared observations, and determine the presence of dew on the vegetation.

Other ancillary data collected during the experiment include:

- Vegetation data composed of a land cover classification and measurements of vegetation water content, ground-based surface reflectance (Landsat and MODIS spectral bands), Leaf Area Index (LAI), and vegetation height. These measurements were made for each type of vegetation occurring in the sampling areas in Yanco and repeated throughout the campaign to capture any change in vegetation cover.
- Soil roughness measurements and textural analysis data.

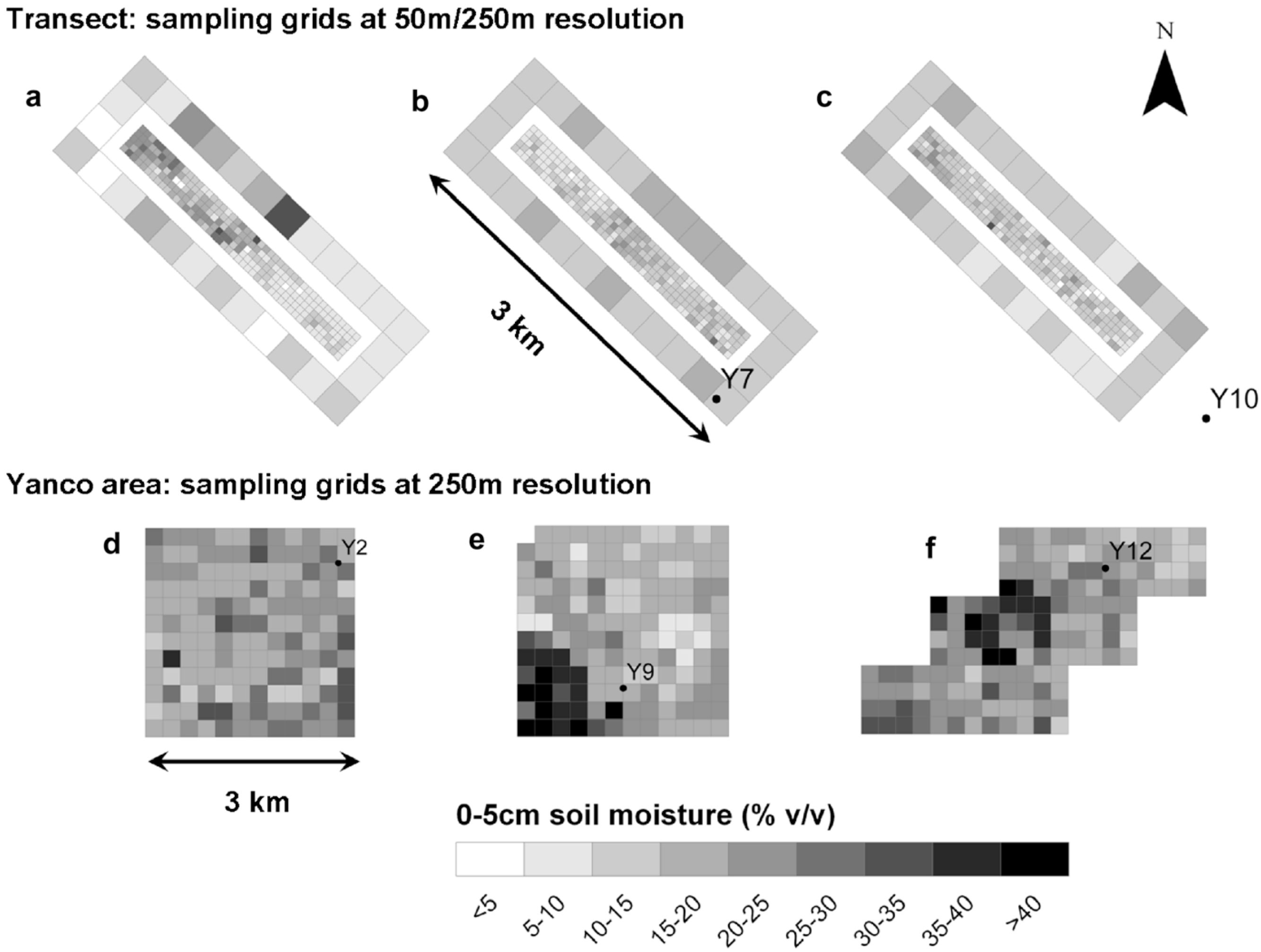

Fig. 5. Sample of spatial 0–5 cm soil moisture ground measurements on 15 November (a: Y1; b: Y7; c: Y10) and 13 November (d: Y2; e:Y9; f:Y12).

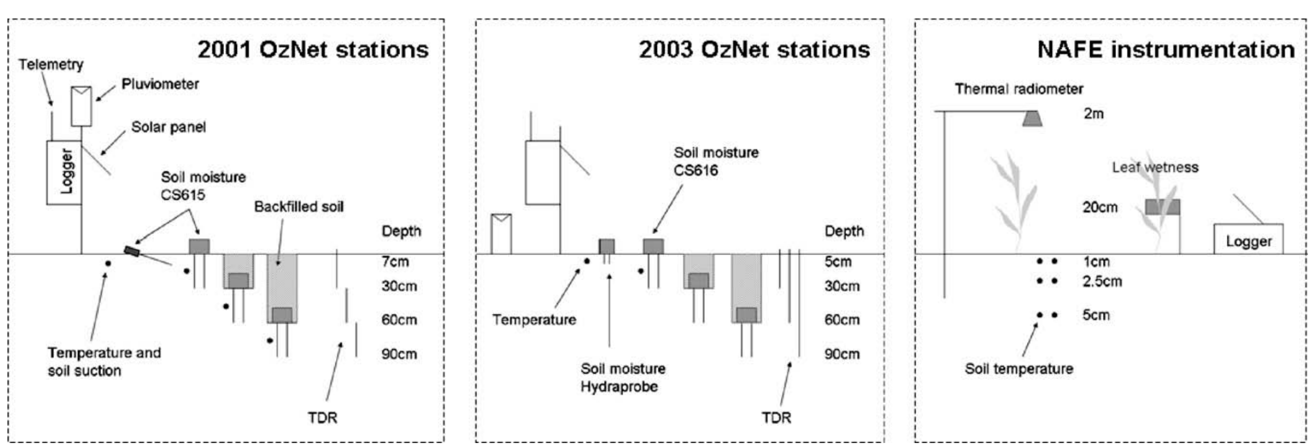

Fig. 6. Schematic of the Murrumbidgee experimental catchment monitoring instrumentation located at soil moisture sites (OzNet). Also shown is the additional NAFE instrumentation located at the sampling farms.

- Surface fluxes monitored by one Eddy flux tower at K10 (Kyeamba), one Bowen ratio near K6 (Livingstone), and three Bowen ratios in the vines at Yenda. The time series of latent heat flux (LE) and sensible heat flux (H) measured at K10 during NAFE'06 are presented in Fig. 7.
- Micro-meteorological data (air temperature, solar radiation, relative humidity and wind speed) collected at two locations in the Yanco area and two locations in the Kyeamba area (see Fig. 1), two stations being operated by the Bureau of Meteorology.

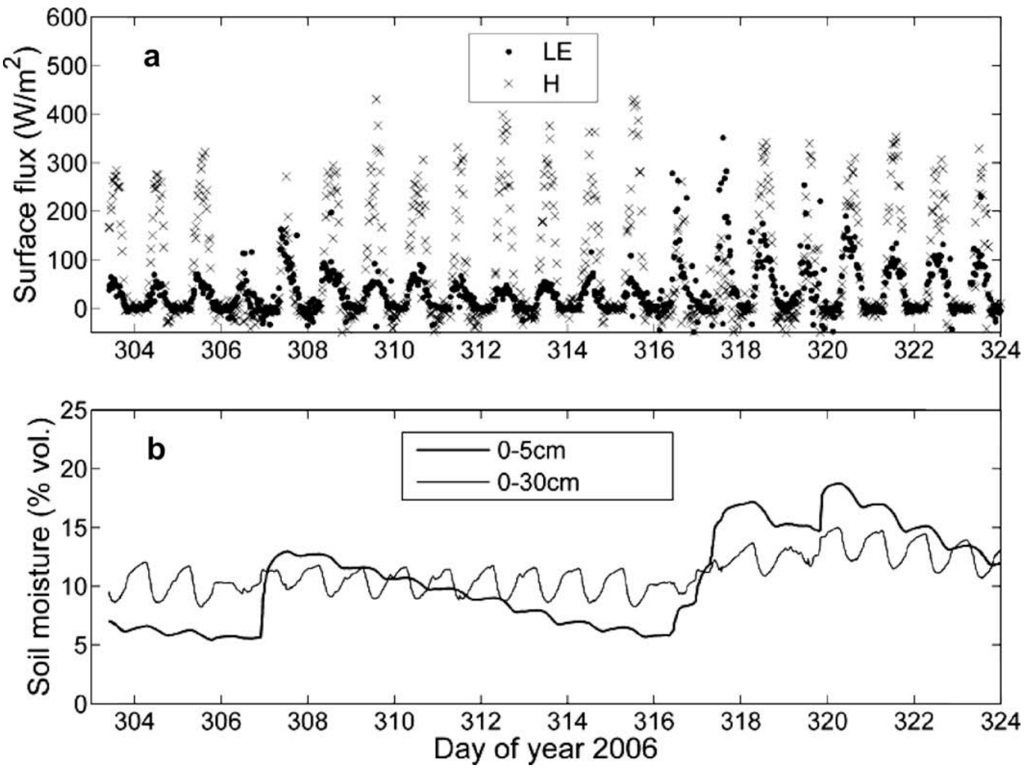

Fig. 7. Example of surface fluxes and soil moisture time series data collected at K10 for period 30 October to 20 November 2006.

4. Towards 1 km resolution soil moisture

In this section, preliminary results from NAFE'06 are presented to assess the accuracy and sensitivity of ground, airborne and satellite data at 1 km scale.

4.1. Ground measurements: accuracy and representative scale

One of the concerns of NAFE'06 was assessment of the accuracy of the 0–5 cm soil moisture measurements undertaken in Yanco and their representativeness at 1 km scale. In order to address this, an average of 3 HDAS readings were made with less than 1 m separation at each node of the sampling grids. The standard deviation computed for each of the ~ 3200 measurement points with more than three independent measurements is plotted against the average in Fig. 8a. As the standard deviation with only three values is not statistically meaningful, results are averaged over 5% vol. bins. Results indicate that the variability of point-scale measurements increases with the mean up to about 5% vol. and then decreases slowly down to 3% vol. in saturated soils, with the maximum variability being reached at 30% vol. The same trend is also observed by selecting the measurement points (125 points) where more than five independent measurements were made. Note that the higher variability obtained with more than five measurements is partly explained by the sampling strategy: more than three measurements were made where the variability was found to be high.

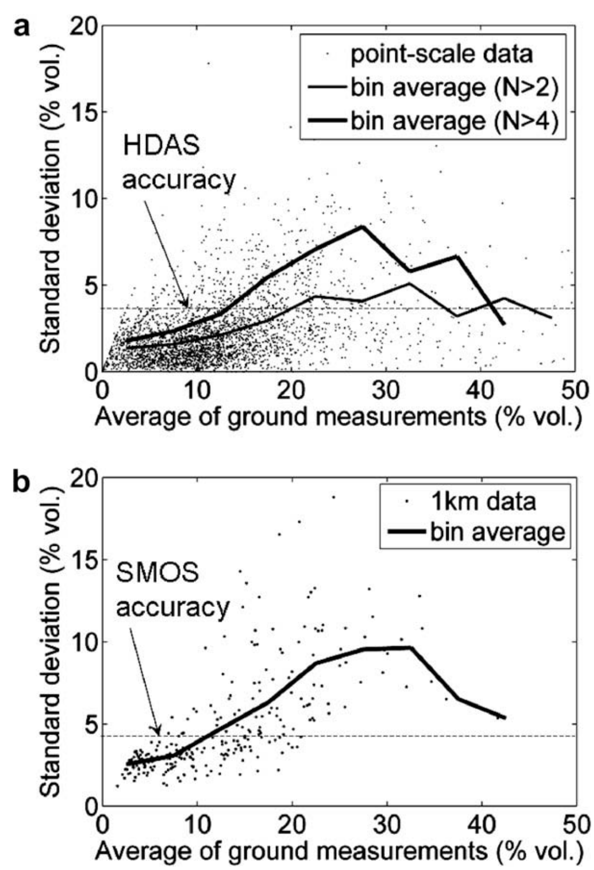

Fig. 8. Standard deviation versus mean of ground measurements evaluated at (a) point scale and (b) 1 km scale for all data collected from the six farms in Yanco. In (a), results are presented for a number of independent measurements (N) of at least 3, and at least 5.

To evaluate the representativeness of point-scale measurements at the aircraft resolution, the standard deviation of the ground measurements within 1 km resolution areas is plotted against the average in Fig. 8b. The (captured) variability of soil moisture increases up to 10% vol. and then decreases to 5% vol. at saturation, with the maximum variability being reached at about 30% vol. Consequently, a similar behaviour is therefore observed at both point and 1 km-scales, with a maximum variability (5% vol. for 1 m and 10% vol. for 1 km) higher than the accuracy of the sensor (3.5% for HDAS and 4% vol. for SMOS) reached at about 30% vol.

The representativeness of ground measurements can also be assessed by comparing the 1 km averages with PLMR data. For each 1 km resolution PLMR pixel falling into the sampling areas, the average of ground measurements is evaluated and compared to the brightness temperature of Fig. 2. By comparing the plots in Fig. 9, it is apparent that the high uncertainty found in some ground data also exists in the comparison with PLMR data, regardless of the number of ground measurements. The correlation coefficient between brightness temperature and ground measurement is 0.67, 0.64, 0.61 for all PLMR pixels, the PLMR pixels including at least 10 ground measurements, and the PLMR pixels including at least 40 ground measurements respectively. However, a significant increase of the correlation coefficient (0.82) is obtained by selecting in Fig. 9d the pixels for which the variability of ground measurements was lower than the point-scale uncertainty.

4.2. PLMR and MODIS soil moisture sensitivity

A first step towards a rigorous analysis of remote sensing data versus soil moisture is to assess the sensitivity of 1 km resolution PLMR brightness temperature and MODIS surface temperature to surface soil moisture for the bare soil and the maximum vegetation cover cases. The data collected on 31 October (very dry) and on 3 November (following the first rainfall event) are used to compare the correlations between MODIS surface temperature and (i) MODIS Normalized Difference Vegetation Index (NDVI) and (ii) PLMR brightness temperature.

Fig. 10 illustrates the "polygonal" correlation between surface temperature and NDVI. Each edge of the polygon can be interpreted as a minimum/maximum reached by vegetation cover (NDVI) and soil moisture [1]. Surface temperature decreases with an increasing NDVI, and for a given NDVI the surface temperature decreases with an increasing soil wetness. The surface temperature-NDVI space obtained on 31 October and 3 November is consistent with previous analyses under non-energy-limited conditions (e.g. [17]) and relatively low vegetation covers.

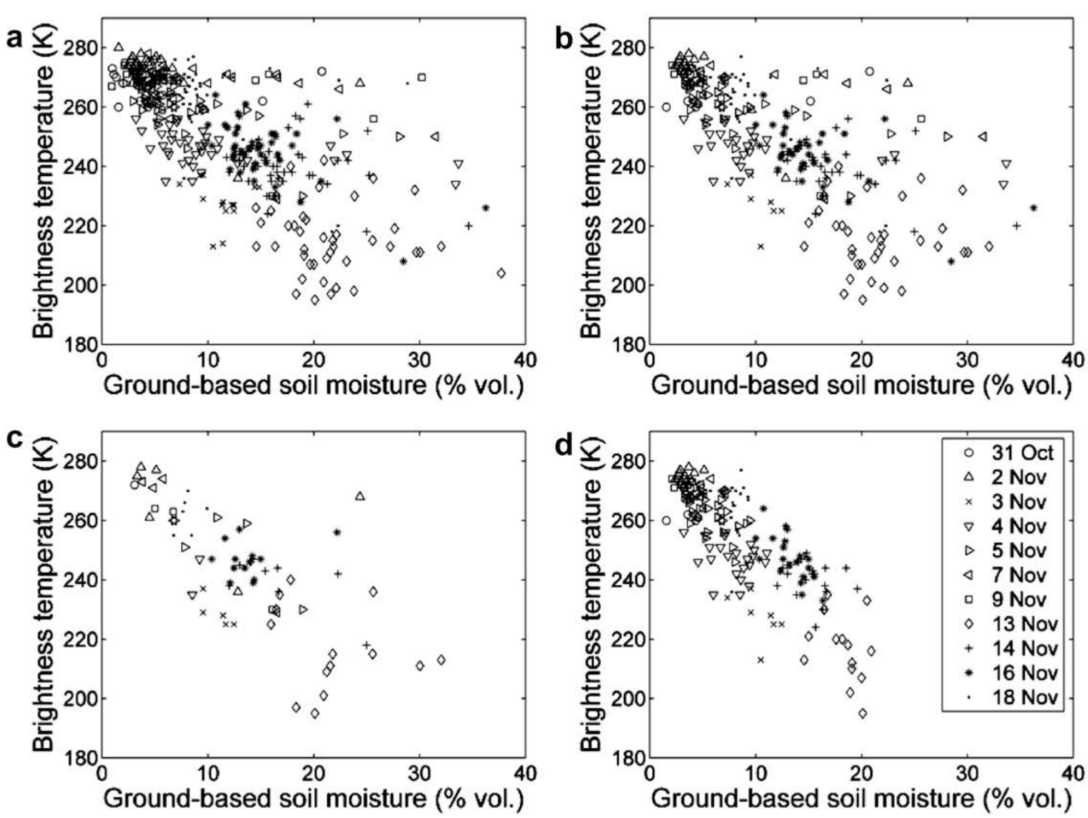

Fig. 9. PLMR data versus ground measurements of 0–5 cm soil moisture at 1 km resolution with (a) the whole data set, (b) the pixels with at least 10 measurements, (c) the pixels with at least 40 measurements and (d) the pixels with at least 10 measurements with a variance lower than 5% vol.

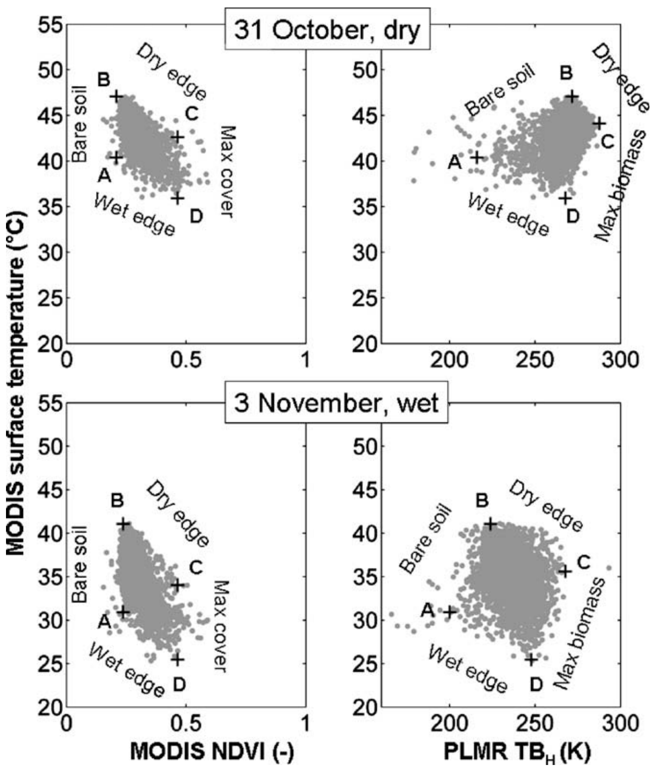

Fig. 10. Sensitivity of (a) MODIS surface temperature and (b) PLMR brightness temperature to soil wetness and vegetation cover on 31 October (dry) and 3 November (wet).

Fig. 10 also shows the "polygonal" correlation obtained between surface temperature and L-band brightness temperature. The longest side of the polygon is the bare soil edge (AB), which illustrates the high sensitivity of L-band brightness temperature to soil moisture over bare soils. On the dry edge (from B to C), the brightness temperature increases while the surface temperature decreases and the NDVI increases. This is consistent with the fact that the different effects of vegetation generally result in an increase of brightness temperature compared to the bare soil case [10]. On the maximum biomass edge (from C to D), brightness temperature decreases with an increasing soil moisture but the range is much smaller than that with bare soil, which illustrates the loss of soil moisture sensitivity with an increasing vegetation biomass. On the wet edge (from D to A), the brightness temperature decreases with a decreasing biomass, as the contribution of the soil emission in the total surface emission becomes more important. The shape of the polygons obtained under dry (31 October) and wet (3 November) conditions is similar. However, the vegetation impact on brightness temperature (edge B–C) is significantly higher after the rainfall event, probably due to a sudden increase in vegetation wetness and/or the presence of rain interception [16].

The superiority of passive microwave versus thermal infrared to monitor soil moisture does not need to be demonstrated any more [7]. However, the synergy between multi-spectral data still needs to be better understood to make full use of available data. The complementarity of passive microwave and optical data, as illustrated in this simple analysis, can potentially be exploited to derive soil moisture products at improved accuracy (multi-spectral retrieval) and spatial resolution (downscaling). Note that the effect of surface temperature and the presence of irrigation water in the CIA on brightness temperature were not removed in this analysis. These approximations were justified by the strong correlation between PLMR and ground soil moisture data observed in Fig. 9. For SMOS, these factors (standing water, surface temperature) and a number of others (soil texture, salinity, roughness, etc.) will be accounted for using state-of-the-art radiative transfer models and ancillary data [28].

5. Summary

The airborne and ground data set of the NAFE'06 campaign were presented. This extensive field campaign was the result of the collaborative effort of a number of Australian, European and American institutions.

Airborne observations included L-band acquisitions at 1 km resolution over two $\sim$ 40 km wide sites at a time frequency of 1–3 days. Both sites have mixed land use that include standing water in Yanco (rice cropping) and urban areas in Kyeamba (the city of Wagga Wagga). Multi-resolution, multi-angle and multi-spectral airborne data including surface temperature, surface reflectance, lidar data and aerial photos were also collected over selected areas. Airborne data were supported by ground measurements of near-surface soil moisture spatial variability and soil moisture profile temporal change.

Preliminary results from NAFE'06 indicated that (i) the uncertainty of a single measurement was typically less than 5% vol. (ii) the spatial variability of ground measurements at 1 km resolution was up to 10% vol. and (iii) the validation of 1 km resolution PLMR data is facilitated by selecting pixels with a soil moisture variability lower than the point-scale uncertainty, which represented about 70% of the pixels falling into the sampling areas. The possibility of exploiting the synergy of passive microwave and optical data for soil moisture monitoring at improved accuracy and resolution was also illustrated by comparing the sensitivity of 1 km resolution PLMR and MODIS data on a dry and wet day.

This provides a unique data set for addressing science questions related to the operational use of SMOS, including multi-angular and multi-spectral retrieval, mixed pixel retrieval, downscaling and the assimilation into land surface models for root-zone soil moisture retrieval.

6. Data availability

The data described in this paper are available from the world wide web site hosted at www.nafe.unimelb.edu.au. The website provides all the information needed for interpretation of these data, along with site overviews, photographs, data plots and related publications. Due acknowledgement in any publication or presentation arising from use of these data is required.

Acknowledgements

The Yanco farmers involved in the field experiment, Wayne Durnan, David Gooden, Adrian Hays, Franck McKersie, Murray Shaw, and Danean Smith, are gratefully acknowledged. Likewise the landholders of the Livingstone Creek and Yenda site are acknowledged for access to their properties. Coleambally Irrigation Co-operative Limited is also acknowledged for their logistical support in the preparation of the ground sampling. We wish to thank the NAFE'06 participants, Elizabeth Botha, Gilles Boulet, Micah Bell, Aaron Berg, Shakti Chakravarty, Yunming Chen, Evan Christen, Richard de Jeu, Clara Draper, Carmen Gomez, Dionne Hansen, Ruud Hurkmans, Jon Johanson, Vadim Kuzmin, Venkat Lakshmi, Philippe Maisongrande, Lynn McKee, Iva Mladenova, Peggy O'Neill, Walter Rawls, Victor Shoemark, Ryan Teuling, Mark Thyer, and Jessika Toyra. The National Airborne Field Experiments have been made possible through recent infrastructure (LE0453434 and LE0560930) and research (DP0557543) funding from the Australian Research Council, and the collaboration of a large number of scientists from throughout Australia, United States and Europe. Initial setup and maintenance of the study catchments was funded by a research grant (DP0343778) from the Australian Research Council and by the CRC for Catchment Hydrology.

References

[1] Carlson TN, Gillies RR, Schmugge TJ. An interpretation of methodologies for indirect measurement of soil water content. Agric For Meteorol 1995;77:191–205.

[2] Crow WT, Ryu D, Famiglietti JS. Upscaling of field-scale soil moisture measurements using distributed land surface modeling. Adv Water Resour 2005;28(1):1–14.

[3] de Rosnay P, Calvet J-C, Kerr Y, Wigneron J-P, Lemaître F, Escorihuela MJ, et al. SMOSREX: a long term field campaign experiment for soil moisture and land surface processes remote sensing. Remote Sens Environ 2006;102:377–89.

[4] Entekhabi D, Nakamura H, Njoku EG. Solving the inverse problem for soil moisture and temperature profiles by sequential assimilation of multifrequency remotely sensed observations. IEEE Trans Geosci Remote Sens 1994;32(2):438–48.

[5] Grayson RB, Western AW. Towards areal estimation of soil water content from point measurements: time and space stability of mean response. J Hydrol 1998;207:68–82.

[6] Jackson TJ, Vine DML, Hsu AY, Oldak A, Starks PJ, Swift CT, et al. Soil moisture mapping at regional scales using microwave radiometry: the southern great plains hydrology experiment. IEEE Trans Geosci Remote Sens 1999;37(5):2136–51.

[7] Kerr YH. Soil moisture from space: where are we? Hydrogeol J 2007;15:117–20.

[8] Kerr YH, Waldteufel P, Wigneron J-P, Martinuzzi J-M, Font J, Berger M. Soil moisture retrieval from space: the soil moisture and ocean salinity (SMOS) mission. IEEE Trans Geosci Remote Sens 2001;39:1729–35.

[9] Kim G, Barros AP. Downscaling of remotely sensed soil moisture with a modified fractal interpolation method using contraction mapping and ancillary data. Remote Sens Environ 2002;83:400–13.

[10] Kim Y, van Zyl J. Vegetation effects on soil moisture estimation. In: J Geosci and Remote Sens symposium, vol. 2; 2004. p. 800–2.

[11] Merlin O, Chehbouni G, Kerr Y, Goodrich D. A downscaling method for distributing surface soil moisture within a microwave pixel: Application to the Monsoon'90 data. Remote Sens Environ 2006;101:379–89.

[12] Merlin O, Walker J, Panciera R, Young R, Kalma J, Kim E. Soil moisture measurement in heterogeneous terrain. In: MODelling and SIMulation Society of Australia and New Zealand. New Zealand; 2007.

[13] Panciera R, Merlin O, Young R, Walker JP. The hydraprobe data acquisition system (HDAS): user guide. University of Melbourne, Report; 2006.

[14] Panciera R, Walker JP, Kalma JD, Kim EJ, Hacker JM, Merlin O, et al. The NAFE'05/CoSMOS data set: toward SMOS calibration, downscaling and assimilation. IEEE Trans Geosci Remote Sens 2008;46(3):736–45.

[15] Rüdiger C, editor. Streamflow data assimilation for soil moisture prediction. The University of Melbourne, Australia, PhD thesis; 2007.

[16] Saleh K, Wigneron J-P, de Rosnay P, Calvet J-C, Escorihuela MJ, Kerr Y, et al. Impact of rain interception by vegetation and mulch on the L-band emission of natural grass. Remote Sens Environ 2006;101:127–39.

[17] Sandholt I, Rasmussen K, Andersen J. A simple interpretation of the surface temperature/vegetation index space for assessment of surface moisture status. Remote Sens Environ 2002;79:213–24.

[18] Schmugge T, Jackson TJ, Kustas WP, Wang JR. Passive microwave remote sensing of soil moisture: results from HAPEX, FIFE and MONSOON'90. J Photogram Remote Sens 1992;47:127–43.

[19] Schwank M, Mätzler C, Guglielmetti M, Flühler H. L-band radiometer measurements of soil water under growing clover grass. IEEE Trans Geosci Remote Sens 2005;43(10):2225–37.

[20] Seyfried MS, Grant LE, Du E, Kumes K. Dielectric loss and calibration of the hydra probe soil water sensor. Vadose Zone 2005;4:1070–9.

[21] Summerell GK, Vaze J, Tuteja NK, Grayson RB, Beale G, Dowling TI. Delineating the major landforms of catchments using an objective hydrological terrain analysis method. Water Resour Res 2005;41:W12416.

[22] Timbal B, Power S, Colman R, Viviand J, Lirola S. Does soil moisture influence climate variability and predictability over Australia? J Clim 2002;15:1230–8.

[23] van Neil TG, McVicar TR, Fang H, Liang S. Calculating environmental moisture for per-field discrimination of rice crops. Int J Remote Sens 2003;24(4):885–90.

[24] Wagner W, Bloschl G, Pampaloni P, Calvet J-C, Bizzari B, Wigneron J-P, et al. Operational readiness of microwave remote sensing of soil moisture for hydrologic applications. Nordic Hydrol 2007;38(1):1–20.

[25] Walker JP, Willgoose GR, Kalma JD. One-dimensional soil moisture profile retrieval by assimilation of near-surface observations. Adv Water Resour 2001;24(6):631–50.

[26] Western A, Seyfried MS. A calibration and temperature correction procedure for the water-content reflectometer. Hydrol Proc 2005;19(18):3785–93.

[27] Western AW, Zhou S-L, Grayson RB, McMahon TA, Bloschl G, Wilson DJ. Spatial correlation of soil moisture in small catchments and its relationship to dominant spatial hydrological processes. J Hydrol 2004;286:113–34.

[28] Wigneron J-P, Kerr Y, Waldteufel P, Saleh K, Escorihuela M-J, Richaume P, et al. L-band microwave emission of the biosphere (L-MEB) model: description and calibration against experimental data sets over crop fields. Remote Sens Environ 2007;107(4):639–55.

[29] Wigneron J-P, Waldteufel P, Chanzy A, Calvet J-C, Kerr Y. Two-dimensional microwave interferometer retrieval capabilities over land surfaces (SMOS mission). Remote Sens Environ 2000;73:270–82.